NIH Public Access
Author Manuscript
*J Biol Rhythms*. Author manuscript; available in PMC 2008 September 16.

Published in final edited form as:
*J Biol Rhythms*. 2008 August ; 23(4): 296–307. doi:10.1177/0748730408318588.

# The blue light photoreceptor CRYPTOCHROME is expressed in a subset of circadian oscillator neurons in the *Drosophila* CNS

**Juliana Benito**[2,3], **Jerry H. Houl**[1,2], **Gregg W. Roman**[2], and **Paul E. Hardin**[1]

1*Department of Biology and Center for Research on Biological Clocks, Texas A&M University, 3258 TAMU, College Station, TX 77843−3258*

2*Department of Biology and Biochemistry, University of Houston, 4800 Calhoun, Houston, TX 77204−5001*.

## Abstract

In the fruit fly *Drosophila melanogaster*, CRYPTOCHROME (CRY) functions as a photoreceptor to entrain circadian oscillators to light-dark cycles and as a transcription factor to maintain circadian oscillator function in certain peripheral tissues. Given the importance of CRY to circadian clock function, we expected this protein to be expressed in all oscillator cells, yet CRY cellular distribution and subcellular localization has not been firmly established. Here we investigate CRY spatial expression in the brain using a newly developed CRY antibody and a novel set of *cry* deletion mutants. We find that CRY is expressed in s-$LN_v$s, l-$LN_v$s and a subset of $LN_d$s and $DN_1$s, but not $DN_2$s and $DN_3$s. CRY is present in both the nucleus and cytoplasm of these neurons, and its subcellular localization does not change over the circadian cycle. Although CRY is absent in $DN_2$s and $DN_3$s, *cry* promoter activity and/or *cry* mRNA accumulation can be detected in these neurons, suggesting that CRY levels are regulated post-transcriptionally. Oscillators in $DN_2$s and $DN_3$s entrain to environmental light-dark cycles, which implies that they are entrained indirectly by retinal photoreceptors, extra-retinal photoreceptors or other CRY expressing cells.

### Keywords

circadian clock; cryptochrome; Drosophila; immunolocalization; behavior; mutant

## Introduction

The fruit fly *Drosophila melanogaster* keeps circadian time via interlocked *period*/*timeless* (*per*/*tim*) and *Clock* (*Clk*) transcriptional feedback loops (reviewed in Hardin 2005). These feedback loops operate in the brain and many peripheral tissues to control behavioral, physiological and metabolic rhythms. Several groups of oscillator neurons in the lateral and dorsal brain control rhythms in locomotor activity (Helfrich-Forster 2005; Shafer et al. 2006). Oscillator neurons in the lateral brain include the dorsal lateral neurons ($LN_d$s), the large ventral lateral neurons (l-$LN_v$s), small ventral lateral neurons (s-$LN_v$s), and the lateral posterior neurons (LPNs). The s-$LN_v$s are further subdivided into four cells that express the neuropeptide Pigment Dispersing Factor (PDF), and a fifth s-$LN_v$ that lacks PDF expression (the $5^{th}$ s-$LN_v$). Three additional clusters of oscillator neurons reside in the dorsal brain: dorsal neurons 1s ($DN_1$s), $DN_2$s and $DN_3$s. The s-LNvs are sufficient for locomotor activity rhythms in

Corresponding author: Paul E. Hardin, Department of Biology, Texas A&M University, 3258 TAMU, College Station, TX 77843−3258; Phone: 979−458−4478; Fax: 979−845−2891; e-mail: phardin@mail.bio.tamu.edu.
[3]Present address: Department of Experimental Therapeutics, The University of Texas MD Anderson Cancer Center, 1515 Holcombe Blvd., Houston, TX 77030

NIH-PA Author Manuscript
NIH-PA Author Manuscript
NIH-PA Author Manuscript

NIH-PA Author Manuscript

NIH-PA Author Manuscript

NIH-PA Author Manuscript

constant darkness (DD), whereas in 12h light: 12h dark (LD) conditions s-$LN_v$s control the morning peak of activity, and the $5^{th}$ s-$LN_v$ and the $LN_d$s control the evening peak of activity (Grima et al. 2004; Rieger et al. 2006; Stoleru et al. 2004). Peripheral tissues that contain oscillators include sensory organs (e.g. compound eyes, ocelli, antennae, proboscis), testes, the gut, and Malpighian tubules (reviewed in Bell-Pedersen et al. 2005; Hall 2003). Oscillators in olfactory sensory neurons control rhythms in olfactory physiology (Krishnan et al. 1999; Tanoue et al. 2004), but rhythmic outputs from other peripheral oscillator tissues have not been characterized.

Circadian oscillators in the brain and peripheral tissues are entrained by environmental light-dark cycles. Photic entrainment in *Drosophila* is mediated by the blue light photoreceptor CRYPTOCHYROME (CRY), a conserved pterin/flavin containing protein found in other eukaryotes (Cashmore et al. 1999), and photoreceptors in compound eyes, ocelli and the Hofbauer-Buchner eyelet (Helfrich-Forster et al. 2001; Rieger et al. 2003; Veleri et al. 2007). CRY entrains the circadian oscillator by undergoing a light-dependent conformational change that promotes CRY-TIM binding, TIM ubiquitination, and ultimately the proteosome-mediated degradation of TIM (Busza et al. 2004; Ceriani et al. 1999; Koh et al. 2006; Lin et al. 2001; Peschel et al. 2006). Eliminating TIM destabilizes PER, which delays or advances the oscillator depending on whether light is presented during the early evening or late night, respectively. Consequently, mutants that alter or eliminate CRY show severe defects in their entrainment to light (Dolezelova et al. 2007; Emery et al. 2000b; Stanewsky et al. 1998).

In addition to its role as a circadian photoreceptor, CRY is necessary for circadian oscillator function in some peripheral tissues. In antennae, rhythms in *per* and *tim* expression and odor-dependent electroantennagram (EAG) responses are severely disrupted in $cry^b$ mutant flies (Krishnan et al. 2001; Levine et al. 2002). Likewise, rhythmic PER and TIM accumulation in compound eyes and Malpighian tubules are abolished in $cry^b$ flies (Ivanchenko et al. 2001; Stanewsky et al. 1998). Genes activated by CLK-CYC are expressed at high levels in $cry^b$ flies and low levels in flies that overexpress CRY, which suggests that CRY represses CLK-CYC dependent transcription (Collins et al. 2006). Such a role in transcriptional repression is consistent with CRY function in mammals, where transcriptional activation by CLOCK-BMAL1 (the mammalian homolog of CLK-CYC) is repressed by mCry1 and mCry2 (Kume et al. 1999).

The dual roles of CRY as a circadian photoreceptor and, in many peripheral tissues, a transcriptional repressor implies that *cry* expression will encompass all oscillator cells. Several methods have been used to track *cry* expression in the brains (primarily) of adults including *cry* promoter driven Gal4 (*cry*-Gal4) reporter genes (Emery et al. 2000b; Klarsfeld et al. 2004; Zhao et al. 2003), *cry* RNA in situ hybridization (Egan et al. 1999; Zhao et al. 2003), and CRY immunohistochemistry (Klarsfeld et al. 2004), but disparate results within and between these methods leave no clear consensus on *cry* spatial expression. For instance, *cry*-Gal4 lines containing different amounts of *cry* upstream sequences are expressed in virtually all oscillator neurons in the brain and many peripheral tissues (Zheng et al., submitted), whereas *cry*-Gal4 lines that contain the first intron have a more restricted distribution (Emery et al. 2000b; Zheng et al., submitted). Moreover, different insertion sites of the same *cry*-Gal4 construct can produce substantial differences in spatial expression (Zhao et al. 2003). Among all *cry*-Gal4 lines the only common sites of expression are the $LN_v$s and $LN_d$s, though most *cry*-Gal4 lines are also expressed in subsets of $DN_1$s and $DN_3$s (Emery et al. 2000b; Helfrich-Forster et al. 2007; Klarsfeld et al. 2004; Shafer et al. 2006; Stoleru et al. 2004; Zhao et al. 2003). In situ hybridization experiments varied substantially in the number and location of *cry* positive cells, though at maximum *cry* signal was detected in $LN_v$s, $LN_d$s, $DN_2$s and a subset of $DN_1$s (Zhao et al. 2003). A novel peptide antibody detected strong CRY immunostaining in s-$LN_v$s and two $DN_1$s from adult brains, and weaker staining in l-$LN_v$s,

NIH-PA Author Manuscript

NIH-PA Author Manuscript

NIH-PA Author Manuscript

$LN_d$s and additional $DN_1$s (Klarsfeld et al. 2004). In these neurons, CRY was detected in both the cytoplasm and nucleus, but time dependent changes in subcellular localization were not assessed. A weakness of previous *cry* mRNA and protein localization studies was the lack of a negative control in the form of a *cry* null mutant, though such a mutant was recently generated (Dolezelova et al. 2007).

Here we generate a novel CRY antiserum and *cry* deletion mutants to investigate CRY spatial expression and subcellular localization in adult brains. CRY immunostaining is detected in the $LN_v$s and a subset of $LN_d$s and $DN_1$s, but not $DN_2$s or $DN_3$s from wild-type flies, or any oscillator cells in $cry^b$ mutant and *cry* deletion controls. CRY is detected in both the nucleus and cytoplasm at all times of the circadian cycle even though its light dependent molecular target, TIM, translocates from the cytoplasm to the nucleus during the night. These results reveal that CRY is only expressed in a subset of brain oscillator cells, indicating that some oscillator cells entrain to light indirectly. CRY is absent in $DN_2$s and $DN_3$s even though *cry* promoter activity and/or *cry* mRNA are detected in these neurons, suggesting that *cry* is under post-transcriptional control in $DN_2$s and $DN_3$s.

## Materials and Methods

### Fly stocks and transgenic flies

Flies that were wild-type with regard to clock function were either Canton-S or $w^{1118}$. The $cyc^{01}$, $per^{01}$, *tim*-Gal4, $cry^b$, and *hscry* strains have been described previously (Emery et al. 1998; Hazelrigg et al. 1984; Konopka and Benzer 1971; Park et al. 2000; Rutila et al. 1998; Stanewsky et al. 1998). $cry^{b+}$ flies, which are wild-type flies having the same genetic background as $cry^b$ mutants, were generously provided by Dr. R. Stanewsky (School of Biological and Chemical Sciences Queen Mary College, University of London). Flies bearing the P-element P{XP}$cry^{d10630}$ (BL 19331) were obtained from the Bloomington Stock Center (Wilson et al. 2008). All fly strains were reared on medium containing corn meal, molasses, yeast, agar, and Tegosept (a mold inhibitor) at 25°C.

### Generation and characterization of *cry* excisions

To generate *cry* deletions via imprecise excision, P{XP}$cry^{d10630}$, a $w^+$ transposable element insert 57bp upstream of the *cry* transcription start site, was excised as described (Greenspan 2004). The approximate size of deletions due to imprecise excision was determined by PCR. To precisely determine the deletion endpoints in three different excision lines, PCR products containing the deleted sequences were cloned into pCR-Blunt II-TOPO vector (Invitrogen). For A2, the primer combination used was cryjumpF 5'-ATCTTTTCTCGCAGCCATTAT-3' and cryjumpR5 5'-CGATATTCAGCTCCCGACAT-3', and for B1 and I1 the primers used were cryjumpF3 5'-CCTGGCGTATGGGTAAGTG-3' with cryjumpR5. Inserts for each of the deletions were sequenced on both strands.

### Fly heat shock

*hs-cry* flies were placed in an empty vial, pushing the cotton lid down so that the flies were close to the bottom. The vial was incubated on a 37°C water bath for 30 minutes. Immediately after that, flies were transferred to a 25 °C dark incubator, recovered for 2hr, collected and stored at −80 °C.

### CRY antibody generation

Full length CRY was expressed in *E. coli*, purified and used to produce antisera in Guinea pigs. A DNA fragment containing the complete *cry* coding region was amplified from a head cDNA library (Hamilton'91) using the crypETs1 (5' GGAATTCACATATGGCCACGCGAGG 3')

NIH-PA Author Manuscript

NIH-PA Author Manuscript

NIH-PA Author Manuscript

and crypETa1 (GGAATTCACTCGAGTCAAACCACCACGTC 3') primers. This fragment was inserted into the *Nco*I and *Xho*I sites of pET28a (+) to generate pET28a-*cry*, which expresses an N-terminal HIS-tagged CRY fusion protein. pET28a-*cry* was transformed into BL21 cells and protein expression was induced using IPTG. CRY fusion protein was purified from cell lysates using a copper affinity column (Amersham) as described (Houl et al. 2006). A single band at the predicted molecular weight of the CRY fusion protein (~60kDa) was detected, and used to immunize guinea pigs for antibody production (Cocalico Biological Inc).

## Whole mount immunofluorescence

Flies were entrained in a 12 hour Light: 12 hour Dark cycle (LD) for at least three days, released into constant darkness (DD), and collected at the indicated time points. Adult brains were dissected in 1XPBS pH7.4 followed by fixation with 5% formaldehyde in 0.1M Phosphate buffer during 20 min at room temperature. The specimens were then washed twice with 1xPBS (10 minutes each), and once with PBT (1XPBS pH7.4, 0.05% Triton-X100) for 10 minutes. Blocking was performed with 5% goat serum, 2% BSA in PBT at room temperature for 3hr or at 4°C O/N. Primary antibody dilutions were prepared in 2% goat serum in PBT, added to the brains, and incubated at 4°C for at least 48 hours. Dilutions used for the primary antibodies were 1/300 for rabbit anti PER that was preadsorbed against $per^{01}$ (Cheng and Hardin 1998), 1/1000 for rabbit anti PDF, and 1/100 for guinea pig anti CRY. Brains were left for 2 hr at room temperature before washing off the primary antibody with PBT for at least 6 times (30 minutes each) at room temperature. Specimens were incubated with fluorescently labeled secondary antibody (1:300) diluted in PBT at 4°C overnight. Secondary antibodies used were: Alexa Fluor 488 goat anti-rabbit and Alexa Fluor 488 and 568 goat anti-guinea pig (Molecular Probes, Invitrogen), Cy3 goat anti-rabbit and Cy3 goat anti-guinea pig (Jackson ImmunoResearch Laboratories Inc.). After equilibration for 2 hr at room temperature, brains were washed with PBT for 30 minutes at least 6 times at room temperature and mounted on glass slides using Vectashield (Vectorlab). Visualization of whole mounts was performed using an Olympus FV100 confocal microscope. Serial Z-stack images were obtained at 1−2um intervals. Images were processed using Adobe Photoshop. Images shown in the figures are overlays of several confocal stacks or single optical sections.

## Behavioral analysis

Locomotor activity was assessed using Drosophila Activity Monitors (TriKinetics Inc.). Flies were entrained in LD cycles at 25°C for 3 days and then kept in constant darkness or constant light for at least 7 days. The data collected was analyzed with Fly Activity Analysis Suite for Mac OSX (FaasX), version 0.7.1 (Copyright 2002−2003 Boudinot, CNRS-INAF). Flies having powers >10 and widths >2 were considered rhythmic.

## Real time PCR

*cry* mRNA levels were assayed by Quantitative Real Time PCR (RT-PCR). Flies were entrained in a 12hour light: 12hour dark cycle for at least three days and collected at Zeitgeiber Time (ZT) 5 and ZT17 (where ZT0 corresponds to lights on and ZT12 to lights off). Total RNA was isolated from fly heads using TRIZOL (Invitrogen). To eliminate genomic DNA contamination, each sample was treated with DNase (Promega). First-strand cDNA was synthesized from 2ug of RNA using random primers and Superscript™ II (Invitrogen) in an Eppendorf Mastercycler® gradient (Eppendorf). *Ribosomal protein 49* (*rp49*) was used as the internal control. Reactions were carried out on an ABI Prism® 7000 Sequence Detector System (ABI). The sequences of the primers and probes used for the different messages are: *cry* forward 5'-CACCGCTGACCTACCAAA-3', *cry* reverse 5'-GGTGGAAGCCCAATAATTTGC-3', *cry* probe 5'6 FAM- TGTTCCTGCACACGGT-3'MGBNFQ; rp49 forward 5'-CTGCCCACCGGATTCAAG-3', rp49 reverse 5'-CGATCTCGCCGCAGTAAAC-3', rp49

NIH-PA Author Manuscript

NIH-PA Author Manuscript

NIH-PA Author Manuscript

probe 5'VIC-CCTCCAGCTCGCGCACGTTG-3'MGBNFQ. For mRNA quantification, a standard curve was prepared for *cry* and *rp49*. Target mRNAs and *rp49* relative values were calculated based on the standard curve and the studied mRNA values were normalized to *rp49*.

### Western blots

During the initial western blot experiments, head extracts were prepared as described (Emery et al. 1998), and blots were developed for chemiluminescence using ECL (Amersham). Subsequently, head extracts were prepared by homogenizing heads from ~50 flies in 3 volumes of EB4 buffer (5mM Tris-HCl pH 7.5, 50mM KCl, 10mM HEPES pH 7.5, 10% Glycerol, 1mM EDTA, 1mM DTT, 0.05%Triton X100, 0.5mM PMSF, 0.01mg/ml Aprotinin, 0.01mg/ml Leupepetin, 0.002 mg/ml Pepstatin) using sterile pestles, centrifuged at 4°C for 15 minutes, and protein levels in the supernatant were quantified using the DC Protein Assay (Bio-Rad) or the Coomassie (Bradford) Protein Assay Kit (Pierce). 40−60 μg of protein per sample was separated on a 12% acrylamide gel, transferred to nitrocellulose, and blots were developed for chemiluminescence using Advanced Plus ECL (Amersham). Nitrocellulose membranes were blocked in 5% skim milk (or 2% blocking powder if using Advanced Plus ECL) for 1 hr at room temperature or overnight at 4°C, and incubated with 1:5000 dilution of CRY antiserum (or a dilution of 1:7500 for Advanced Plus ECL) overnight at room temperature. Blots were washed six times for 1 hr using 0.1% Tween 20 in TBS (TBST), and incubated with secondary antibody (HRP goat anti-guinea pig, SIGMA) diluted 1/1000 (for detection using ECL) or 1/5000 (for detection using Advanced Plus ECL) in blocking solution for 1 hr at room temperature. Blots were then washed six times for 1 hr in TBST, developed, and exposed to film.

## Results

### Generation of a CRY antibody (* Place Fig. 1 here, 3 inches high)

Full length HIS-tagged CRY protein was produced in bacteria, purified, and used to immunize Guinea pigs. One antiserum, designated GP23, detected a protein of approximately 60 KDa on western blots that was induced to high levels in *hs-cry* flies upon heat shock, which suggests that this protein corresponds to CRY (Fig. 1A). CRY is destabilized by both light and the $cry^b$ mutation (Emery et al. 1998;Stanewsky et al. 1998). After entrainment in LD, wild-type flies were given a 6hr light pulse on the third day of DD and collected at CT18 along with untreated controls. GP23 detected a strong band at ~60kDa in control flies kept in DD, but this band was virtually eliminated after light treatment (Fig. 1B), consistent with detection of CRY. Likewise, when flies were collected every four hours during LD, the band corresponding to CRY rose to high levels during the night and fell to low levels by the end of the day (Fig. 1C). This band was detected at very low levels in $cry^b$ flies (Fig. 1C), further demonstrating that it corresponds to CRY. Consistent with a very long half-life for CRY in DD, the band detected by GP23 accumulates during the first day of DD (Fig. 1D).

### Generation and confirmation of *cry* null mutants (* Place Fig. 2 here, 1 column wide)

Most functional studies of CRY are based on the $cry^b$ mutant, which produces low levels of CRY that retain some CRY activity (Dolezelova et al. 2007; Emery et al. 1998; Stanewsky et al. 1998). However, $cry^b$ may not serve as a useful negative control for immunolocalization studies since CRY antisera may detect the low levels of $CRY^b$ protein. To avoid this potential problem, mutants having no detectable CRY expression were generated via imprecise P-element excisions (see Materials and Methods). Of 16 precise excision and 30 *cry* deletion lines, one precise excision line (B2) and seven deletion lines were selected for further characterization. The abundance of *cry* mRNA was measured in these eight lines at times when *cry* mRNA was at peak (ZT5) and trough (ZT17) levels. In the wild-type and B2 controls,

NIH-PA Author Manuscript

NIH-PA Author Manuscript

NIH-PA Author Manuscript

*cry* mRNA is expressed at ~2-fold higher levels at ZT5 than ZT17 (Fig. 2A). In contrast, *cry* mRNA from the seven deletion strains ranged from undetectable to 4-fold lower than *cry* mRNA in wild-type and B2 flies at ZT17 or *cry* mRNA in $cry^b$ flies at ZT5 and ZT17 (Fig. 2A). Consistent with these *cry* mRNA results, CRY levels were very low or undetectable in the seven deletion strains and $cry^b$, but were high in wild-type and B2 flies (Fig. 2B). These results argue that the seven *cry* deletion strains examined are either null or severely hypomorphic.

Three lines that produce extremely low levels of *cry* mRNA, A2, B1 and I1, were characterized in detail. The A2 deletion removed 50bp of *cry* upstream sequence and 963bp of *cry* transcribed sequence, the B1 deletion removed 835bp *cry* upstream sequence and 881bp of *cry* transcribed sequence, and the I1 deletion removed 1209bp of *cry* upstream sequence and 1279bp of *cry* transcribed sequence (Fig. 2C). In each case, the deleted sequences remove the *cry* transcription and translation initiation sites, consistent with the loss of *cry* mRNA and protein expression in these strains. We will refer to these new *cry* alleles as $cry^{\Delta A2}$, $cry^{\Delta B1}$ and $cry^{\Delta I1}$. (* Place Table 1 here, 1 column wide)

The loss of CRY function in $cry^b$ flies enables rhythmic behavioral activity with slightly long periods in constant light and disrupts phase shifts to pulses of light (Emery et al. 2000a; Emery et al. 2000b; Stanewsky et al. 1998). Nevertheless, robust circadian activity rhythms with ~24hr periods in $cry^b$ flies indicates that *cry* is not required for oscillator function in neurons that mediate locomotor activity rhythms (Stanewsky et al. 1998). To determine whether the behavioral phenotypes of the $cry^{\Delta A2}$, $cry^{\Delta B1}$ and $cry^{\Delta I1}$ mutants are similar to, or more severe than, $cry^b$, we tested behavioral rhythms under LL and DD conditions after entrainment in LD. Wild-type and B2 control flies were arrhythmic in LL, while ~85% of $cry^b$ flies were rhythmic with a period of 25.4hr (Table 1). Like $cry^b$ flies, ~70% to 90% of $cry^{\Delta A2}$, $cry^{\Delta B1}$ and $cry^{\Delta I1}$ flies exhibited rhythmic locomotor activity under LL having periods of ~25hr (Table 1). Under DD conditions, $cry^{\Delta A2}$, $cry^{\Delta B1}$ and $cry^{\Delta I1}$ flies were mostly rhythmic with periods of ~24.5 −25.5hr., which was similar to the B2 control flies having the same genetic background, but longer period than either the wild-type or $cry^b$ controls (Table 2). The similarity in LL and DD locomotor activity phenotypes between $cry^b$ and the *cry* deletion lines suggests that $cry^{\Delta A2}$, $cry^{\Delta B1}$ and $cry^{\Delta I1}$ are severely hypomorphic or null. (* Place Table 2 here, 1 column wide)

## CRY localization in adult brains (* Place Fig. 3 here, 5 inches high)

In situ hybridization and promoter analyses show that *cry* is expressed almost exclusively in brain oscillator cells, though the number and identity oscillator cells that express *cry* vary among studies (Emery et al. 2000b; Zhao et al. 2003; Zheng et al., submitted). To determine whether GP23 can detect CRY expression in oscillator cells, we used this antibody along with antiserum against the clock cell marker PER to immunostain brains from flies collected at CT19 on the third day of DD. Strong CRY immunoreactivity (CRY-IR) was detected in many, but not all PER expressing brain neurons (Fig. 3A-C). A magnified image of the lateral brain region shows CRY-IR in all of the s-$LN_v$s, l-$LN_v$s, and some $LN_d$s (Fig. 3B). In the dorsal brain region, CRY-IR is detected in a majority of the $DN_1$s, but not in $DN_2$s or $DN_3$s (Fig 3C). Two of the $DN_1$s show more intense CRY-IR than other DN1s, and likely correspond to $DN_1$a neurons based on their position (Shafer et al. 2006). CRY-IR was uniform within all CRY positive oscillator neurons, suggesting that CRY is present in both the cytoplasm and the nucleus at this time. Projections from oscillator neurons also showed CRY-IR (Fig. 3C), consistent with previous results (Klarsfeld et al. 2004). However, CRY-IR could only be detected in neuronal projections from flies kept for at least 3 days in DD, suggesting that such staining is due to inordinately high levels of CRY that have accumulated over several days. CRY-IR is also detected in non-PER expressing cells in the Pars Intercerebralis (PI) and medial

NIH-PA Author Manuscript

NIH-PA Author Manuscript

NIH-PA Author Manuscript

protocerebrum (Fig. 3D). These cells were quite large, and CRY-IR was cytoplasmic. (* Place Fig. 4 here, 5 inches high)

To confirm that CRY-IR in adult brains corresponds to CRY, GP23 and PER were used to immunostain brains from $cry^{\Delta I1}$ adults collected on the fourth day of DD. No CRY-IR was detected in neurons that were immunostained with PER (Fig. 4A). However, large PER negative cells in the PI and medial protocerebrum of $cry^{\Delta I1}$ flies continued to show CRY-IR similar to that in wild-type flies (Fig. 4B), indicating that this immunostaining is non-specific. Brains from $cry^{\Delta A2}$ and control B2 excision flies collected on the third day of DD were immunostained with PDF and GP23 antisera to confirm the lack of CRY-IR in $LN_v$s using a separate *cry* deletion strain. Although CRY-IR was seen in $LN_v$s from B2 controls, no CRY-IR was detected in $LN_v$s from $cry^{\Delta A2}$ flies (Fig. 4C). In addition, no CRY-IR was detected in oscillator cells from $cry^{b}$ flies collected on the third day of DD (Fig. 4D). The lack of CRY-IR in $cry^{\Delta A2}$, $cry^{\Delta I1}$, and $cry^{b}$ flies demonstrates that GP23 specifically detects CRY.

### Localization of CRY in brain oscillator neurons during the circadian cycle (* Place Fig. 5 here, 5 inches high)

Since TIM localization shifts from the cytoplasm to the nucleus during the night and is degraded during the morning (Hunter-Ensor et al. 1996; Meyer et al. 2006; Myers et al. 1996; Shafer et al. 2002; Zeng et al. 1996), it is possible that CRY undergoes similar changes in subcellular localization so that it can always access TIM. To test this possibility, brains from flies collected every 4hr during the third day of DD were immunostained with PER and CRY antisera. Consistent with previous results (Shafer et al. 2002; Veleri et al. 2003; Yang and Sehgal 2001), high amplitude rhythms in PER abundance and nuclear localization were seen in s-$LN_v$s, $LN_d$s and $DN_1$s, but not l-$LN_v$s (Fig. 5A). However, CRY abundance and subcellular localization to both the nucleus and cytoplasm were constant in s-$LN_v$s, l-$LN_v$s, $LN_d$s, and $DN_1$s. Constant levels of CRY in l-$LN_v$s and s-$LN_v$s is supported by experiments using PDF as a cytoplasmic marker; CRY abundance and subcellular localization do not cycle in PDF positive cells during the third day of DD (Fig. 5B). These results demonstrate that in brain oscillator neurons, the levels and subcellular localization of CRY remain constant in DD.

## Discussion

### CRY expression in brain oscillator cells

Here we employed a novel CRY antibody and newly generated *cry* deletion mutants to define the pattern of CRY expression in adult brains. CRY immunostaining was detected in most, but not all, groups of oscillator neurons in the adult brain. Specifically, CRY is present in all of the s-$LN_v$s, l-$LN_v$s, but only about half of the $LN_d$s and $DN_1$s, and none of the $DN_2$s or $DN_3$s (Fig. 3AD). Our CRY immunostaining results are consistent with those of Klarsfeld et al., in which CRY-IR could be detected in $LN_v$s, and some $LN_d$s and $DN_1$s on the third day of DD, but not $DN_2$s or $DN_3$s (Klarsfeld et al. 2004). We also detect CRY immunostaining in s-$LN_v$ projections into the dorsal brain. The significance of this observation is not known, but it is likely this staining is simply a consequence of high CRY accumulation in DD over several days since we did not observe such staining under LD cycling conditions (data not shown).

The lack of CRY expression in half the $DN_1$s, and all $DN_2$s and $DN_3$s suggests that the oscillator in these neurons is light-entrained indirectly by other CRY expressing neurons, retinal photoreceptors in the compound eye or ocelli, or extraretinal photoreceptors in the Hofbauer-Buchner eyelet. When retinal and extraretinal photoreceptors are removed using the $gl^{60j}$ mutant, oscillator function persists in $DN_2$s, demonstrating that $DN_2$ oscillators are not light-entrained by retinal or extraretinal photoreceptors (Helfrich-Forster et al. 2001). However, in $cry^{b}$ flies oscillator function is lost in $DN_2$s, suggesting that these neurons entrain indirectly

NIH-PA Author Manuscript

NIH-PA Author Manuscript

NIH-PA Author Manuscript

through other CRY expressing neurons (Helfrich-Forster et al. 2001). Since s-$LN_v$s are not able to reset oscillator phase in $DN_2$s (Stoleru et al. 2005), other CRY expressing neurons must entrain $DN_2$s.

We expected *cry* mRNA to be expressed in all CRY-expressing brain cells. However, different *cry* promoter driven Gal4 lines (with or without *cry* intron 1) give variable patterns of GFP reporter gene (i.e. UAS-GFP) expression, with some lines expressing exclusively in a single cluster of brain oscillator neurons, and others expressing in most or all of the brain oscillator neuron clusters along with different groups of non-oscillator cells (Emery et al. 2000b; Klarsfeld et al. 2004; Zhao et al. 2003). Recent analysis of different portions of the *cry* promoter (with or without the first intron) driving Gal4 show consistent expression of a β-galactosidase (i.e. UAS-lacZ) reporter gene within all six clusters of brain oscillator neurons (Zheng et al., submitted). In situ hybridization analysis detects *cry* mRNA in all three groups of LNs, $DN_1$s and $DN_2$s, but not $DN_3$s (Zhao et al. 2003). Since *cry*-Gal4 driven reporter genes and *cry* RNA in situ hybridizations detect *cry* expression in s-$LN_v$s, l-$LN_v$s, $LN_d$s and $DN_1$s, it is not surprising that CRY is present in these neuronal clusters. However, we do not detect CRY in $DN_2$s even though *cry* expression can be detected via reporter gene and RNA in situ analyses. Similarly, CRY is not detected in a group of non-oscillator cells in the dorsal margin of the optic lobe (DOL cells) that express *cry* mRNA and *cry* promoter dependent reporter genes (Zhao et al. 2003). These results suggest that CRY is either not translated or is unstable in $DN_2$s and DOLs. Although *cry*-Gal4 driven reporter gene expression can be detected in $DN_3$s (Klarsfeld et al. 2004; Zheng et al., submitted), no *cry* mRNA is detected by in situ hybridization (Zhao et al. 2003), indicating that *cry* mRNA is unstable in these cells. Taken together, these studies indicate that *cry* expression is regulated at the transcriptional or post-transcriptional level depending on the cluster of brain oscillator neurons.

CRY-IR was consistently observed in non-oscillator cells within the Pars Intercerebralis (PI), a region of the dorsal protocerebrum containing neurosecretory cells (de Velasco et al. 2007), and the medial protocerebrum. Unlike brain oscillator cells, CRY-IR in these cells was very intense and always cytoplasmic. However, in contrast to a loss of CRY-IR in oscillator cells from $cry^b$ and *cry* deletion flies, CRY-IR remained in the cytoplasm of cells in the PI and medial brain (Fig. 4B), suggesting that CRY-IR in these cells is not due to CRY. These results suggest that the GP23 antibody cross-reacts with a protein present in these cells.

### Subcellular localization of CRY during the circadian cycle

During the circadian cycle, TIM accumulates in the cytoplasm during the early evening, then moves into the nucleus until it is degraded during the early morning (in LD) or the subjective early morning (in DD) (Hunter-Ensor et al. 1996; Meyer et al. 2006; Myers et al. 1996; Shafer et al. 2002; Zeng et al. 1996). However, CRY does not move from the cytoplasm to the nucleus each day, but is present in both the nucleus and cytoplasm at all times of the circadian cycle (Fig. 5A, B). CRY nuclear and cytoplasmic localization provides constant access to TIM, thus allowing for phase resetting in response to light at any time during the circadian cycle. Since CRY controls oscillator function in some peripheral tissues by rhythmically repressing CLK-CYC activity in the nucleus (Collins et al. 2006), it is possible that rhythms in CRY nuclear translocation could occur in peripheral tissues.

## Acknowledgements

We thank P. Emery, R. Stanewsky, J. Hall for providing antibodies or *Drosophila* strains, and C. Helfrich-Forster for communicating results prior to publication. We also thank A. Kralcheva for generating the CRY expression plasmid. This work was supported by NIH grants NS051280 (PEH) and NS042185 (GR).

NIH-PA Author Manuscript

NIH-PA Author Manuscript

NIH-PA Author Manuscript

## References


Bell-Pedersen D, Cassone VM, Earnest DJ, Golden SS, Hardin PE, Thomas TL, Zoran MJ. Circadian rhythms from multiple oscillators: lessons from diverse organisms. Nat Rev Genet 2005;6:544–556. [PubMed: 15951747]

Busza A, Emery-Le M, Rosbash M, Emery P. Roles of the two Drosophila CRYPTOCHROME structural domains in circadian photoreception. Science 2004;304:1503–1506. [PubMed: 15178801]

Cashmore AR, Jarillo JA, Wu YJ, Liu D. Cryptochromes: blue light receptors for plants and animals. Science 1999;284:760–765. [PubMed: 10221900]

Ceriani MF, Darlington TK, Staknis D, Mas P, Petti AA, Weitz CJ, Kay SA. Light-dependent sequestration of TIMELESS by CRYPTOCHROME. Science 1999;285:553–556. [PubMed: 10417378]

Cheng Y, Hardin PE. Drosophila photoreceptors contain an autonomous circadian oscillator that can function without period mRNA cycling. J Neurosci 1998;18:741–750. [PubMed: 9425016]

Collins B, Mazzoni EO, Stanewsky R, Blau J. Drosophila CRYPTOCHROME is a circadian transcriptional repressor. Curr Biol 2006;16:441–449. [PubMed: 16527739]

de Velasco B, Erclik T, Shy D, Sclafani J, Lipshitz H, McInnes R, Hartenstein V. Specification and development of the pars intercerebralis and pars lateralis, neuroendocrine command centers in the Drosophila brain. Dev Biol 2007;302:309–323. [PubMed: 17070515]

Dolezelova E, Dolezel D, Hall JC. Rhythm defects caused by newly engineered null mutations in Drosophila's cryptochrome gene. Genetics 2007;177:329–345. [PubMed: 17720919]

Egan ES, Franklin TM, Hilderbrand-Chae MJ, McNeil GP, Roberts MA, Schroeder AJ, Zhang X, Jackson FR. An Extraretinally Expressed Insect Cryptochrome with Similarity tio the Blue Light Photoreceptors of Mammals and Plants. J Neurosci 1999;19:3665–3673. [PubMed: 10233998]

Emery P, So WV, Kaneko M, Hall JC, Rosbash M. CRY, a *Drosophila* clock and light-regulated cryptochrome, is a major contributor to circadian rhythm resetting and photosensitivity. Cell 1998;95:669–679. [PubMed: 9845369]

Emery P, Stanewsky R, Hall JC, Rosbash M. A unique circadian-rhythm photoreceptor. Nature 2000a; 404:456–457. [PubMed: 10761904]

Emery P, Stanewsky R, Helfrich-Forster C, Emery-Le M, Hall JC, Rosbash M. *Drosophila* CRY is a deep brain circadian photoreceptor. Neuron 2000b;26:493–504. [PubMed: 10839367]

Greenspan, RJ. Fly pushing: The theory and practice of Drosophila genetics. Cold Spring Harbor Press; Cold Spring Harbor: 2004.

Grima B, Chelot E, Xia R, Rouyer F. Morning and evening peaks of activity rely on different clock neurons of the Drosophila brain. Nature 2004;431:869–873. [PubMed: 15483616]

Hall JC. Genetics and molecular biology of rhythms in Drosophila and other insects. Adv Genet 2003;48:1–280. [PubMed: 12593455]

Hardin PE. The circadian timekeeping system of Drosophila. Curr Biol 2005;15:R714–722. [PubMed: 16139204]

Hazelrigg T, Levis R, Rubin GM. Transformation of white locus DNA in drosophila: dosage compensation, zeste interaction, and position effects. Cell 1984;36:469–481. [PubMed: 6319027]

Helfrich-Forster C. Neurobiology of the fruit fly's circadian clock. Genes Brain Behav 2005;4:65–76. [PubMed: 15720403]

Helfrich-Forster C, Shafer OT, Wulbeck C, Grieshaber E, Rieger D, Taghert P. Development and morphology of the clock-gene-expressing lateral neurons of Drosophila melanogaster. J Comp Neurol 2007;500:47–70. [PubMed: 17099895]

Helfrich-Forster C, Winter C, Hofbauer A, Hall JC, Stanewsky R. The circadian clock of fruit flies is blind after elimination of all known photoreceptors. Neuron 2001;30:249–261. [PubMed: 11343659]

Houl JH, Yu W, Dudek SM, Hardin PE. Drosophila CLOCK Is Constitutively Expressed in Circadian Oscillator and Non-Oscillator Cells. J Biol Rhythms 2006;21:93–103. [PubMed: 16603674]

Hunter-Ensor M, Ousley A, Sehgal A. Regulation of the *Drosophila* protein *timeless* suggests a mechanism for resetting the circadian clock by light. Cell 1996;84:677–685. [PubMed: 8625406]

NIH-PA Author Manuscript

NIH-PA Author Manuscript

NIH-PA Author Manuscript

Ivanchenko M, Stanewsky R, Giebultowicz JM. Circadian photoreception in *Drosophila*: functions of *cryptochrome* in peripheral and central clocks. J Biol Rhythms 2001;16:205–215. [PubMed: 11407780]

Klarsfeld A, Malpel S, Michard-Vanhee C, Picot M, Chelot E, Rouyer F. Novel features of cryptochrome-mediated photoreception in the brain circadian clock of Drosophila. J Neurosci 2004;24:1468–1477. [PubMed: 14960620]

Koh K, Zheng X, Sehgal A. JETLAG resets the *Drosophila* circadian clock by promoting light-induced degradation of TIMELESS. Science 2006;312:1809–1812. [PubMed: 16794082]

Konopka RJ, Benzer S. Clock mutants of Drosophila melanogaster. Proc Natl Acad Sci U S A 1971;68:2112–2116. [PubMed: 5002428]

Krishnan B, Dryer SE, Hardin PE. Circadian rhythms in olfactory responses of Drosophila melanogaster. Nature 1999;400:375–378. [PubMed: 10432117]

Krishnan B, Levine JD, Lynch MK, Dowse HB, Funes P, Hall JC, Hardin PE, Dryer SE. A new role for cryptochrome in a *Drosophila* circadian oscillator. Nature 2001;411:313–317. [PubMed: 11357134]

Kume K, Zylka MJ, Sriram S, Shearman LP, Weaver DR, Jin X, Maywood ES, Hastings MH, Reppert SM. mCRY1 and mCRY2 are essential components of the negative limb of the circadian clock feedback loop. Cell 1999;98:193–205. [PubMed: 10428031]

Levine JD, Funes P, Dowse HB, Hall JC. Advanced analysis of a cryptochrome mutation's effects on the robustness and phase of molecular cycles in isolated peripheral tissues of Drosophila. BMC Neurosci 2002;3:5. [PubMed: 11960556]

Lin FJ, Song W, Meyer-Bernstein E, Naidoo N, Sehgal A. Photic signaling by cryptochrome in the *Drosophila* circadian system. Mol Cell Biol 2001;21:7287–7294. [PubMed: 11585911]

Meyer P, Saez L, Young MW. PER-TIM interactions in living Drosophila cells: an interval timer for the circadian clock. Science 2006;311:226–229. [PubMed: 16410523]

Myers MP, Wager-Smith K, Rothenfluh-Hilfiker A, Young MW. Light-induced degradation of TIMELESS and entrainment of the *Drosophila* circadian clock. Science 1996;271:1736–1740. [PubMed: 8596937]

Park JH, Helfrich-Forster C, Lee G, Liu L, Rosbash M, Hall JC. Differential regulation of circadian pacemaker output by separate clock genes in *Drosophila*. Proc Natl Acad Sci U S A 2000;97:3608–3613. [PubMed: 10725392]

Peschel N, Veleri S, Stanewsky R. Veela defines a molecular link between Cryptochrome and Timeless in the light-input pathway to Drosophila's circadian clock. Proc Natl Acad Sci U S A 2006;103:17313–17318. [PubMed: 17068124]

Rieger D, Shafer OT, Tomioka K, Helfrich-Forster C. Functional analysis of circadian pacemaker neurons in Drosophila melanogaster. J Neurosci 2006;26:2531–2543. [PubMed: 16510731]

Rieger D, Stanewsky R, Helfrich-Forster C. Cryptochrome, compound eyes, Hofbauer-Buchner eyelets, and ocelli play different roles in the entrainment and masking pathway of the locomotor activity rhythm in the fruit fly Drosophila melanogaster. J Biol Rhythms 2003;18:377–391. [PubMed: 14582854]

Rutila JE, Suri V, Le M, So WV, Rosbash M, Hall JC. CYCLE is a second bHLHPAS clock protein essential for circadian rhythmicity and transcription of *Drosophila period* and *timeless*. Cell 1998;93:805–814. [PubMed: 9630224]

Shafer OT, Helfrich-Forster C, Renn SC, Taghert PH. Reevaluation of Drosophila melanogaster's neuronal circadian pacemakers reveals new neuronal classes. J Comp Neurol 2006;498:180–193. [PubMed: 16856134]

Shafer OT, Rosbash M, Truman JW. Sequential nuclear accumulation of the clock proteins period and timeless in the pacemaker neurons of Drosophila melanogaster. J Neurosci 2002;22:5946–5954. [PubMed: 12122057]

Stanewsky R, Kaneko M, Emery P, Beretta B, Wager-Smith K, Kay SA, Rosbash M, Hall JC. The *cry*$^{b}$ mutation identifies cryptochrome as a circadian photoreceptor in *Drosophila*. Cell 1998;95:681–692. [PubMed: 9845370]

Stoleru D, Peng Y, Agosto J, Rosbash M. Coupled oscillators control morning and evening locomotor behaviour of Drosophila. Nature 2004;431:862–868. [PubMed: 15483615]

NIH-PA Author Manuscript

NIH-PA Author Manuscript

NIH-PA Author Manuscript

Stoleru D, Peng Y, Nawathean P, Rosbash M. A resetting signal between Drosophila pacemakers synchronizes morning and evening activity. Nature 2005;438:238–242. [PubMed: 16281038]

Tanoue S, Krishnan P, Krishnan B, Dryer SE, Hardin PE. Circadian clocks in antennal neurons are necessary and sufficient for olfaction rhythms in *Drosophila*. Curr Biol 2004;14:638–649. [PubMed: 15084278]

Veleri S, Brandes C, Helfrich-Forster C, Hall JC, Stanewsky R. A self-sustaining, light-entrainable circadian oscillator in the Drosophila brain. Curr Biol 2003;13:1758–1767. [PubMed: 14561400]

Veleri S, Rieger D, Helfrich-Forster C, Stanewsky R. Hofbauer-Buchner eyelet affects circadian photosensitivity and coordinates TIM and PER expression in *Drosophila* clock neurons. J Biol Rhythms 2007;22:29–42. [PubMed: 17229923]

Wilson RJ, Goodman JL, Strelets VB. FlyBase: integration and improvements to query tools. Nucleic Acids Res 2008;36:D588–593. [PubMed: 18160408]

Yang Z, Sehgal A. Role of molecular oscillations in generating behavioral rhythms in *Drosophila*. Neuron 2001;29:453–467. [PubMed: 11239435]

Zeng H, Qian Z, Myers MP, Rosbash M. A light-entrainment mechanism for the *Drosophila* circadian clock. Nature 1996;380:129–135. [PubMed: 8600384]

Zhao J, Kilman VL, Keegan KP, Peng Y, Emery P, Rosbash M, Allada R. *Drosophila* Clock Can Generate Ectopic Circadian Clocks. Cell 2003;113:755–766. [PubMed: 12809606]

NIH-PA Author Manuscript

NIH-PA Author Manuscript

NIH-PA Author Manuscript

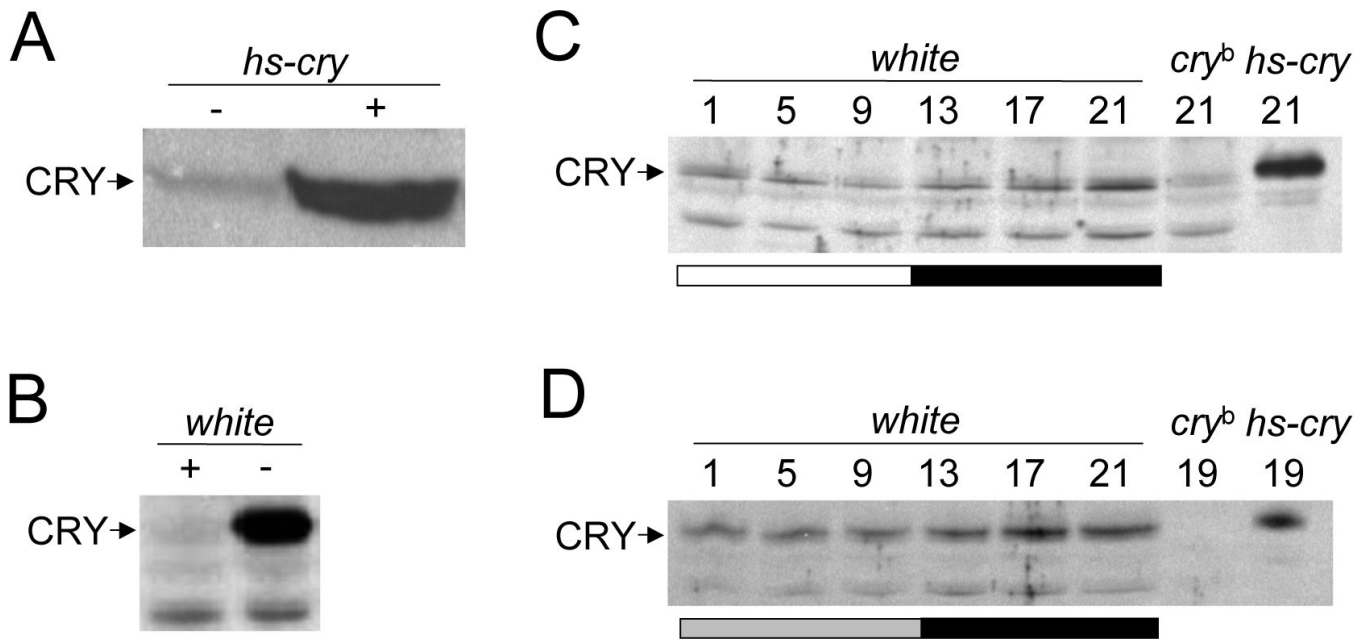


**Figure 1.**

GP23 antiserum detects CRY in fly head extracts. A. Western containing head extracts from *hs-cry* flies that were heat induced (+) or uninduced (−) at 37°C for 30 min. A ~60 kDa band corresponding to CRY is detected. B. Western containing head extracts from wild-type flies that received (+) or did not receive (−) a 6hr light pulse at CT12 on the third day of DD before being collected at CT18. C. Western blot of *white*, *cry*$^{b}$ and heat induced *hs-cry* flies collected at the times shown during a 12hr light: 12hr dark cycle and probed with GP23. The CRY and non-specific (ns) bands are shown. D. Western blot of *white*, *cry*$^{b}$ and heat induced *hs-cry* flies collected at the times shown during the first day of DD and probed with GP23. The CRY band is shown. In panels B-D, proteins were extracted using the lab's standard procedure (see Material and Methods). All experiments were replicated at least three times with similar results.

NIH-PA Author Manuscript

NIH-PA Author Manuscript

NIH-PA Author Manuscript

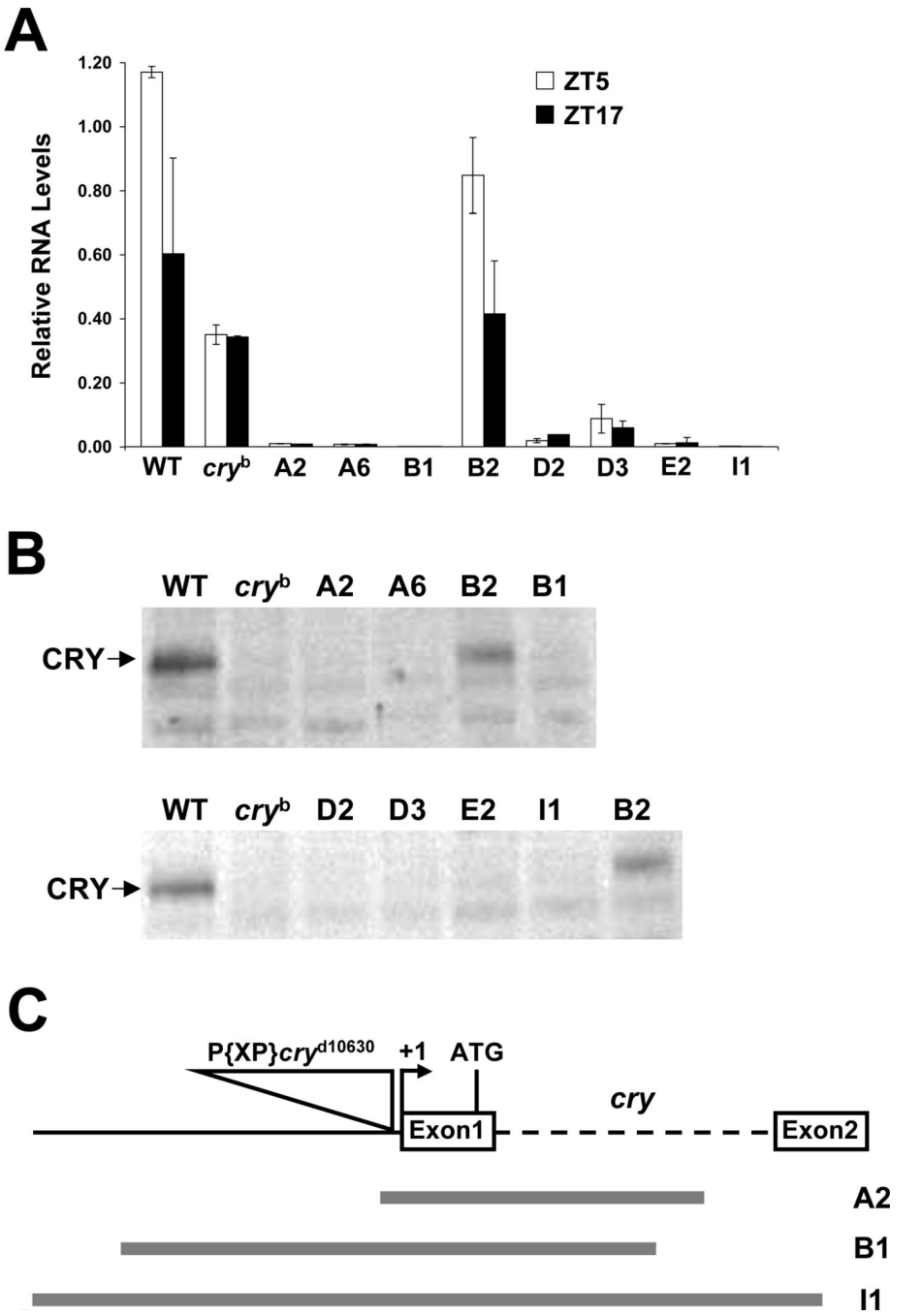


**Figure 2.**

Expression and structure of *cry* deletion mutants. A. qPCR of *cry* mRNA from the heads of *w* (WT), *cry*$^{b}$ and *cry* excision flies (A1, A6, B1, B2, D2, D3, E2, I1) collected at ZT5 (white bars) or ZT17 (black bars) under LD conditions. Relative *cry* mRNA levels were quantified as described in Materials and Methods. Error bars are ±SD. B. Western blots of head extracts from *w* (WT), *cry*$^{b}$ and excision flies (A1, A6, B1, B2, D2, D3, E2, I1) collected at CT19 during the first day of DD were probed with GP23. In panels A and B, B2 is a precise excision control. C. Structural characterization of *cry* deletion mutants. Diagram of the *cry* gene (top) showing the first two exons (white boxes), intron 1 (dashed line), upstream sequence (black line), the

P{XP}*cry*$^{d10630}$ insert (triangle), the transcription start site (+1) and the translation start site (ATG). The extent of deleted sequences the A2, B1 and I1 strains are shown as gray lines.

NIH-PA Author Manuscript
NIH-PA Author Manuscript
NIH-PA Author Manuscript

NIH-PA Author Manuscript
NIH-PA Author Manuscript
NIH-PA Author Manuscript



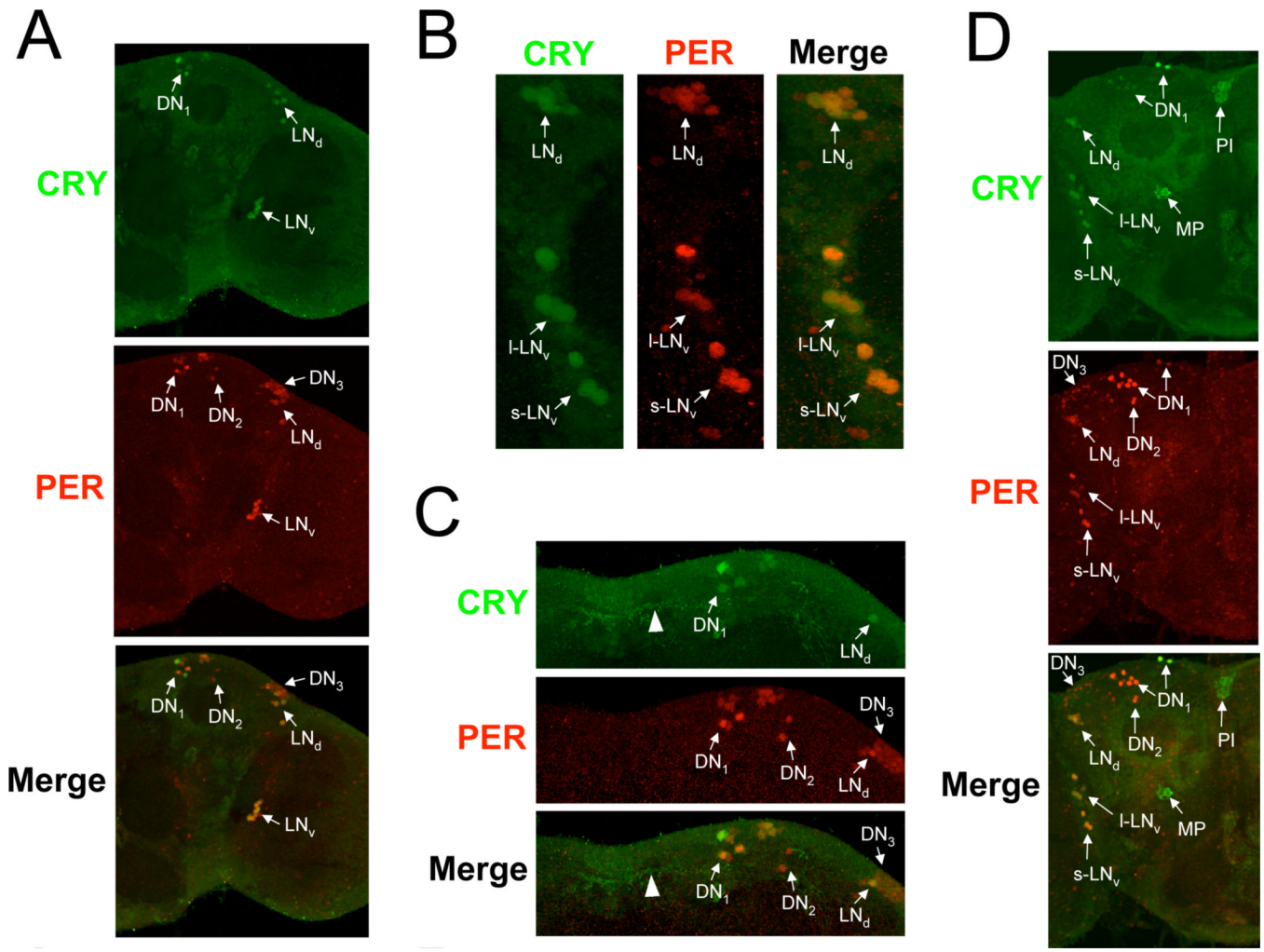


**Figure 3.**

CRY expression in adult brains. Brains were dissected from *w* flies collected at CT19 on the third day of DD, immunostained with CRY (GP23) and PER antisera, and imaged via confocal microscopy. A minimum of six brains were analyzed with similar results. A. Images of a 2μm z-stack projection through the left hemisphere are shown, where dorsal is at the top. Colocalization of CRY (green) and PER (red) immunofluorescence is seen in the merged image as yellow. Arrows indicate CRY and/or PER immunostaining in oscillator neurons. s-$LN_v$, small ventrolateral neurons; l-$LN_v$s, large ventrolateral neurons; $LN_d$s, dorsolateral neurons; DN1, dorsal neuron1s; DN2, dorsal neuron 2s; DN3, dorsal neuron 3s. B. A compressed stack of six 1 μm optical sections through the lateral protocerebrum is shown. Colocalization of CRY (green) and PER (red) immunofluorescence is seen in the merged image as yellow. Arrows indicate CRY and/or PER immunostaining in oscillator neurons. Oscillator neurons are labeled as in panel A. C. A compressed stack of six 1μm optical sections through the dorsal protocerebrum is shown. Colocalization of CRY (green) and PER (red) immunofluorescence is seen in the merged image as yellow. Arrows indicate CRY and/or PER immunostaining in oscillator neurons. Oscillator neurons are labeled as in panel A. D. Images of a 2μm z-stack projection through the right hemisphere are shown, where dorsal is at the top. CRY and PER immunostaining and oscillator cells are as described in panels A-C, CRY-IR is also detected in the Pars Intercerebralus (PI) and the medial protocerebrum (MP).

NIH-PA Author Manuscript
NIH-PA Author Manuscript
NIH-PA Author Manuscript



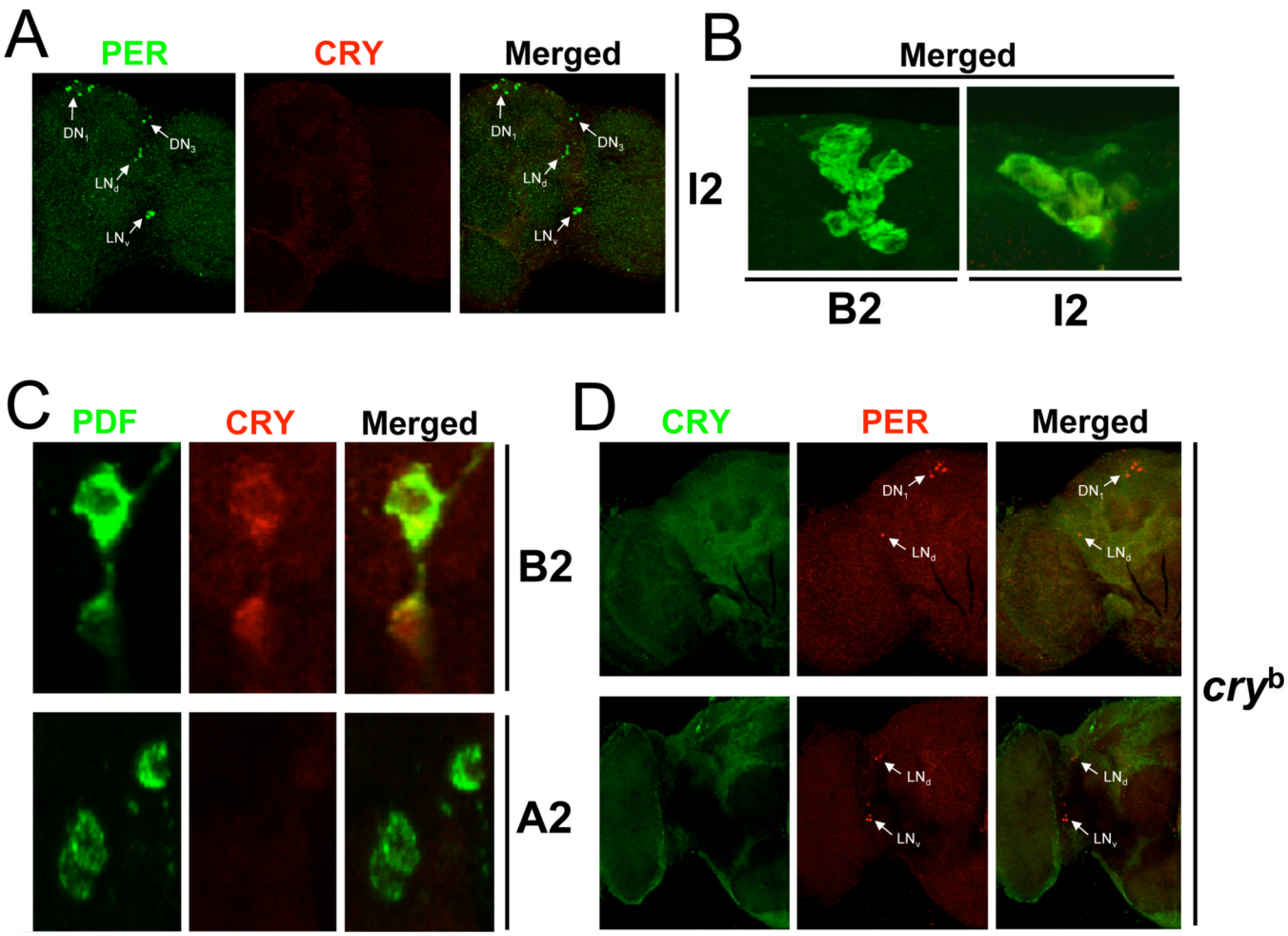


**Figure 4.**

CRY expression in *cry*$^{b}$ and *cry* deletion strains. Brains were dissected from *cry* deletion strains *cry*$^{\Delta I2}$ and *cry*$^{\Delta A2}$, *cry*$^{b}$ mutant flies, and *cry* B2 (precise excision) flies collected at CT19 on the third day of DD, immunostained with CRY (GP23) and PER or PDF antisera, and imaged via confocal microscopy. A minimum of four *cry*$^{\Delta I2}$, four *cry*$^{\Delta A2}$, and six *cry*$^{b}$ brains were analyzed with similar results. A. A 2μm z-stack projection through the left hemisphere of a *cry*$^{\Delta I2}$ fly is shown. Colocalization of PER (green) and CRY (red) immunofluorescence is seen in the merged image as yellow. Arrows indicate PER and/or CRY immunostaining in oscillator neurons, which are labeled as in panel A of Fig. 3. B. A compressed stack of 6−8 1μm optical sections through the Pars Intercerebralus is shown. A merged image of CRY (green) and PER (red) immunofluorescence is shown. C. A compressed stack of 3−6 1μm optical sections through the lateral protocerebrum of *cry* B2 and *cry*$^{\Delta A2}$ flies is shown. Colocalization of PDF (green) and CRY (red) immunofluorescence in s-LN$_v$s is seen in the merged image as yellow. D. A compressed stack of 3−4 2μm optical sections from the right brain hemispheres of *cry*$^{b}$ flies is shown. Colocalization of CRY (green) and PER (red) immunofluorescence in the merged image is shown as yellow. Arrows indicate PER and/or CRY immunostaining in oscillator neurons, which are labeled as in panel A of Fig. 3.

NIH-PA Author Manuscript

NIH-PA Author Manuscript

NIH-PA Author Manuscript

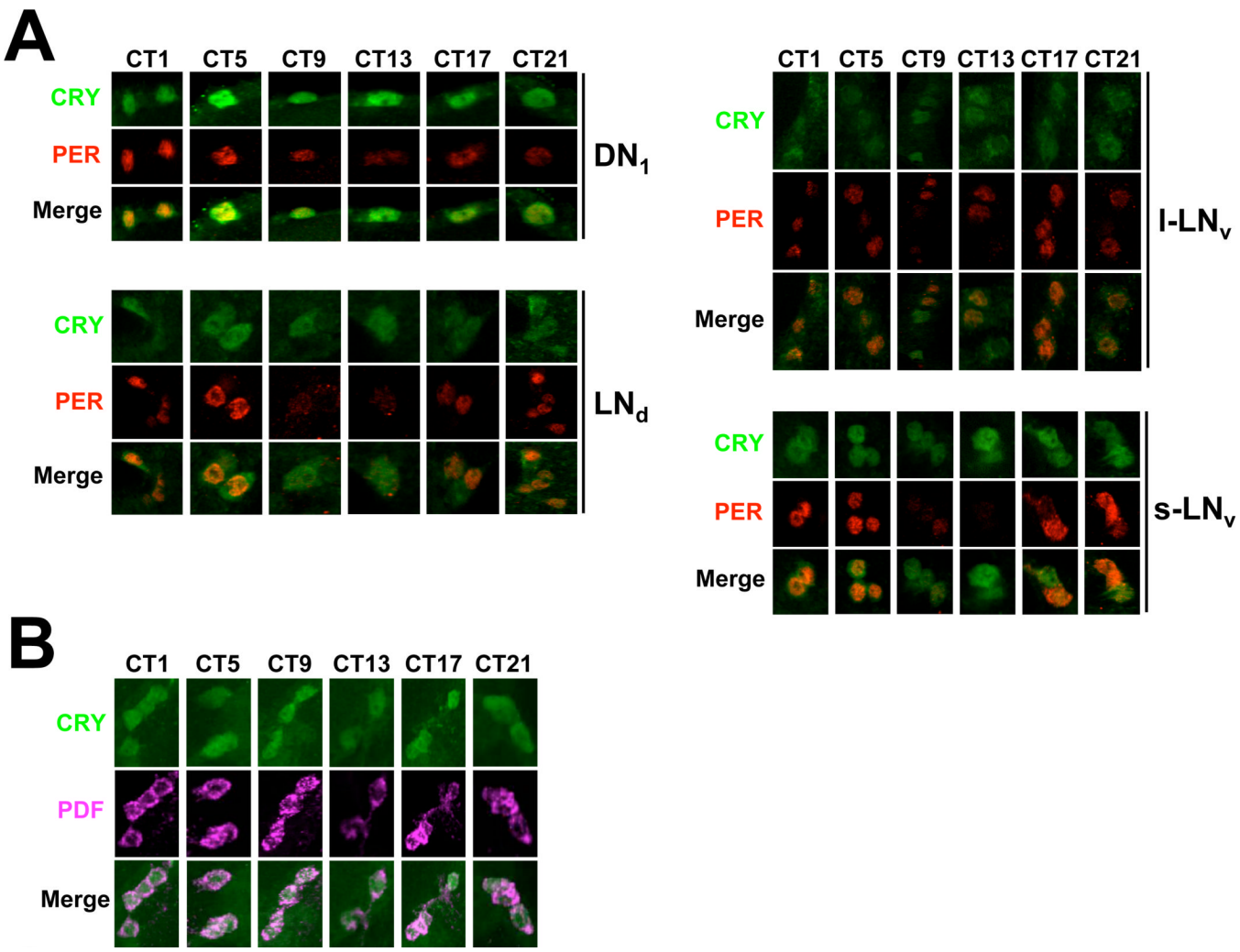


**Figure 5.**

CRY subcellular localization over the circadian cycle. A. Brains were dissected from *w* flies collected every 4 hours starting at CT1 on the third day of DD, immunostained with CRY (GP23) and PER or PDF antisera, and imaged via confocal microscopy. A minimum of five brains were analyzed for each region with similar results. A. 1μm optical sections of $DN_1$s in the dorsal protocerebrum and $LN_d$s, l-$LN_v$s and s-$LN_v$s in the lateral protocerebrum. Colocalization of CRY (green) and PER (red) immunofluorescence is seen in the merged images as yellow. B. A compressed stack of 2−31μm optical sections showing s-$LN_v$s in the lateral protocerebrum. Colocalization of PDF (magenta) and CRY (green) immunofluorescence is seen in the merged image as pink.

NIH-PA Author Manuscript NIH-PA Author Manuscript NIH-PA Author Manuscript



**Table 1**

Locomotor activity rhythms of *cry* excision strains under LL conditions. Period and power were calculated for all rhythmic animals as described in Materials and Methods. Activity was calculated for all flies that survived to the end of the experiment, as described in Materials and Methods. Homozygous deletions are shown in bold. n.a.; not applicable.

| Genotype | N | % Rhythmic (N) | Tau +/−SEM | Power | Activity |
|---|---|---|---|---|---|
| *white* | 16 | 0 | n.a. | n.a. | 22.01+/−2.5 |
| $cry^b$ | 14 | 85.7 (12) | 25.4+/−0.2 | 77.1+/−10.1 | 14.75+/−1.5 |
| *B2/+* | 10 | 0 (0) | n.a. | n.a. | 19.41+/−1.7 |
| *B2/B2* | 17 | 0 (0) | n.a. | n.a. | 24.3+/−2 |
| *A2/+* | 10 | 0 (0) | n.a. | n.a. | 22.01+/−1.4 |
| ***A2/A2*** | **12** | **83.3 (10)** | **25.01+/−0.4** | **42.8+/−7.4** | **30+/−1.4** |
| *B1/+* | 8 | 0 (0) | n.a. | n.a. | 30.2 |
| ***B1/B1*** | **17** | **70.6 (12)** | **26.3+/−0.7** | **50.3+/−8** | **33.7+/−2.4** |
| I1/+ | 11 | 0 (0) | n.a. | n.a. | 22.8+/−1.76 |
| ***I1/I1*** | **20** | **90 (18)** | **25.1+/−0.4** | **51.1+/−7.1** | **25.9+/−2.4** |

NIH-PA Author Manuscript NIH-PA Author Manuscript NIH-PA Author Manuscript



**Table 2**

Locomotor activity rhythms of *cry* excision strains under DD conditions. Period and power were calculated for all rhythmic animals as described in Materials and Methods. Activity was calculated for all flies that survived to the end of the experiment, as described in Materials and Methods. Homozygous deletion strains are shown in bold.

| Genotype | N | %Rhythmic (N) | Tau | Power | Activity |
|---|---|---|---|---|---|
| *white* | 25 | 96 (24) | 23.8+/−0.05 | 93.1+/−7.3 | 26.0+/−1.4 |
| *cry*$^{b}$ | 19 | 74 (14) | 23.9+/−0.09 | 44.5+/−5.9 | 14.1+/−1.7 |
| *B2/+* | 18 | 83.3 (15) | 24.4+/−0.13 | 61.7+/−8.5 | 24.4+/−2.2 |
| *B2/B2* | 29 | 55.2 (16) | 24.8+/−0.11 | 64.77+/−7.9 | 25.7+/−1.7 |
| *B1/+* | 18 | 66.7 (12) | 24.4+/−0.07 | 79+/−18.7 | 21.7+/−1.4 |
| ***B1/B1*** | **19** | **63.2 (12)** | **25.5+/−0.41** | **93.8+/−15.5** | **30.0+/−2.8** |
| *I1/+* | 26 | 88.5 (23) | 24.3+/−0.08 | 50.6+/−6 | 18.8+/−1.6 |
| ***I1/I1*** | **32** | **62.5 (20)** | **24.7+/−0.11** | **61.0+/−4.7** | **27.3+/−1.9** |
| *A2/+* | 14 | 85.7 (12) | 24.6+/−0.18 | 58.2+/−9.8 | 23.3+/−2.1 |
| ***A2/A2*** | **15** | **13.3 (2)** | **24.3+/−0.5** | **18.5+/−3.9** | **23.9+/−2** |